

[Click here to view linked References](#)

Experimental study on a hybrid solar photothermic and radiative cooling collector equipped with a rotatable absorber/emitter plate

Mingke Hu ^a, Bin Zhao ^b, Suhendri ^a, Jingyu Cao ^c, Qiliang Wang ^d, Saffa Riffat ^a, Ronggui Yang ^e,
Yuehong Su ^{a, *}, Gang Pei ^{b, *}

^a *Department of Architecture and Built Environment, University of Nottingham, University Park, Nottingham NG7 2RD, UK*

^b *Department of Thermal Science and Energy Engineering, University of Science and Technology of China, Hefei 230027, China*

^c *College of Civil Engineering, Hunan University, Changsha 410082, China*

^d *Department of Building Services Engineering, The Hong Kong Polytechnic University, Kowloon, Hong Kong, China*

^e *School of Energy and Power Engineering, Huazhong University of Science and Technology, Wuhan 430074, China*

* Corresponding author: yuehong.su@nottingham.ac.uk; peigang@ustc.edu.cn

Abstract

Taking the frigid outer space as the heat sink, a terrestrial body can cool itself to a sub-ambient temperature via radiative sky cooling (RC) scheme. However, poor seasonal and regional adaptabilities and low cooling power density of the RC technology confine its effective applications only in hot seasons and regions with RC-friendly ambient conditions. Similarly, a solar thermal collector cannot work at night and is of little value when heat is needless. To tackle these challenges, a hybrid solar photothermic and radiative cooling (PT-RC) collector equipped with a rotatable absorber/emitter panel is proposed and experimentally investigated. This dual-mode collector can flexibly switch between PT and RC to match specific energy demands in different scenarios. The daily solar thermal efficiency of the PT-RC system at zero-reduced temperature reached 50.4%, a typical level of flat-plate solar water

1 heating systems. The PT-RC system could not provide cooling energy during most daytime hours.
2
3 However, the system could easily achieve nighttime cooling, with the cooling power of the collector
4
5 decreasing from about 60 to 50 W/m² as the circulated water being continuously cooled down from
6
7 around 20 to 12 °C. The average nocturnal cooling power of the PT-RC collector ranged from 30.5 to
8
9 57.5 W/m² in a multi-night RC test. This rotatable PT-RC collector offers a new strategy to flexibly
10
11 deliver heat and coldness in a renewable and environmental-friendly manner and shows the potential
12
13 of smart thermal management in buildings, vehicles, agriculture, etc.
14
15
16
17
18
19

20 **Keywords:** *solar energy; solar collector; radiative cooling; passive cooling; rotatable.*
21
22

23 1. Introduction 24

25
26 Heating and cooling demands in modern society, for example, in the building sector, have been
27
28 expanding significantly, which are responsible for massive energy consumption [1, 2]. Although
29
30 whether human activities such as fossil fuel consumption have caused global warming is still under
31
32 debate [3, 4], it is indisputable that energy shortage has posed a huge challenge to the sustainable
33
34 development of human society. Therefore, further advancing renewable and sustainable energy
35
36 technologies is becoming increasingly imperative. The sun (~5800 K) and the deep universe (~3 K)
37
38 are respectively the natural heat source and sink for the earth, providing renewable energy solutions
39
40 for building energy-saving [5, 6].
41
42
43
44
45
46
47

48
49 Solar thermal collection is a well-handled solar energy technology that has been widely applied in
50
51 domestic water heating [7], space heating [8], crop drying [9], power generation [10], etc. The
52
53 mechanism of solar photothermic (PT) conversion is quite simple; namely, a solar receiver containing
54
55 backside thermal carrier channels traps solar photons that finally dissipate into heat [11]. To achieve
56
57 the highest possible photon-to-thermal conversion efficiency, the receiver should show very high
58
59
60
61
62
63
64
65

1 absorptivity in the whole solar spectrum (i.e., 0.2–3 μm). Meanwhile, the receiver is expected to lose
2
3 minimal thermal energy to hit a higher overall thermal efficiency, which requires the receiving surface
4
5 to present the lowest possible spectral emissivity aside from the solar radiation band (above 3 μm)
6
7 [12]. The well-developed solar selective absorbing coating, usually being coated to the receiver
8
9 substrate through magnetron sputtering [13], physical vapour deposition [14], or electrochemical
10
11 deposition [15], etc., enables the solar receiver to strictly follow the required spectral selectivity and
12
13 to reach a high-level PT efficiency [16].
14
15
16
17
18
19

20 Radiative cooling (RC), on the other hand, is still at its early developing stage either in the research
21
22 or industrial communities, though it was recognized as a passive cooling strategy back to several
23
24 centuries ago [17]. An RC emitter gains cooling energy by radiatively dumping heat to the cold sky
25
26 through the well-known “atmospheric window” lying in between 8 and 13 μm [18]. Quite different
27
28 from the spectral selectivity of a PT absorber, the RC emitter should exhibit high spectral emissivity
29
30 within the “atmospheric window” to strongly dissipate heat to the sky, and simultaneously the emitter
31
32 should show very low spectral absorptivity outside the “atmospheric window” if larger ambient-
33
34 emitter temperature gap is targeted [19, 20]. In particular, given that the cooling load gets higher during
35
36 the daytime with intensive solar radiation in some scenarios (e.g., official buildings, shopping malls),
37
38 RC devices are expected to provide coldness even during peak solar hours [21]. Fortunately, with very
39
40 recent advancements in material sciences and technologies, delivering a spectrally near-ideal RC
41
42 emitter capable of realizing an all-day sub-ambient cooling effect becomes accessible [22, 23].
43
44
45
46
47
48
49
50
51
52

53 Though the PT and RC technologies are two attractive routes to provide renewable thermal energy,
54
55 they still face some challenges and limitations in real-world applications, e.g., building energy-saving.
56
57 The first comes to the inherent low cooling flux of the RC mechanism compared to typical cooling
58
59
60
61
62
63
64
65

1 technologies such as vapor compression refrigeration [24]. The RC flux at room temperature is around
2
3 120 W/m² theoretically, and can easily shrink to half or even less under real circumstances [25], which
4
5 is a huge barrier for widespread use of this cooling technology taking the cost into consideration. The
6
7 second challenge is the poor flexibility of typical stand-alone PT and RC collectors in terms of thermal
8
9 regulation. Unlike the sophisticated all-day RC emitter that can provide cooling energy continuously,
10
11 a spectrally-static solar absorber is out of work at night due to the lack of solar radiation. Such
12
13 operation discontinuity is generally associated with a long pay back period for a solar thermal system.
14
15 Besides, a solar thermal collector cannot provide coldness and may even bring an adverse effect of
16
17 burdening building cooling load on hot days as it will always absorb solar energy when exposed to
18
19 sunlight [26]. Similarly, a spectrally-static RC emitter cannot deliver heat and may even cause an
20
21 undesired cooling effect on cold days, which cannot well match the dynamic energy demands in
22
23 buildings located in four-season regions [27]. Therefore, a solar heater or radiative cooler may be of
24
25 little value in some months of a year in most areas across the world. Such poor seasonal adaptability
26
27 further lowers their running frequency and prolongs the payback period. Considering the commonality
28
29 between PT and RC mechanisms in renewability and extraterrestrial nature, and the complementarity
30
31 concerning their operation periods (hot days vs. cold days, daytime vs. mostly nighttime), types of
32
33 energy outputs (heat vs. coldness), as well as their aforementioned superiorities and practical
34
35 limitations, it is of significance and possibility to integrate them into a single apparatus to increase
36
37 operating availability and provide thermal energy in tune with the specific energy demand.
38
39
40
41
42
43
44
45
46
47
48
49
50
51
52

53 The concept of integrating daytime solar heating and nighttime radiative cooling by applying a
54
55 spectrally-coupled absorber/emitter was firstly introduced by Matsuta et al. [28] and then developed
56
57 by Hu et al. [29, 30]. A hybrid daytime solar heating and nighttime radiative cooling collector shows
58
59
60
61
62
63
64
65

1 the capability of work day and night with better seasonal adaptability, but its daytime solar thermal
2
3 efficiency weakens due to the high emissivity in the “atmospheric window” for radiative cooling. Chen
4
5 et al. [31] deployed a vacuum device to simultaneously conduct solar heating and radiative cooling
6
7 with a mid-infrared transparent solar absorber setting above a radiative emitter, but the stagnation
8
9 temperature of the absorber is only up to 24.4 °C higher than the ambient temperature under intensive
10
11 solar radiation, indicating that the solar thermal performance of the absorber is poor. In fact, for the
12
13 purpose of realizing daytime solar heating and radiative cooling simultaneously, the solar absorber
14
15 temperature should be depressed within a low level to avoid radiating overmuch heat to the radiative
16
17 emitter [32].
18
19
20
21
22
23
24

25 Therefore, combining solar heating and radiative cooling in a single collector but remaining the
26
27 same level of heating and cooling performance is challenging and needs to be further developed. In
28
29 typical solar thermal collectors, the solar absorber panel is structurally fixed and coated by a layer of
30
31 solar selective absorbing coating only on the sun-facing side while leaving the other side untreated and
32
33 untapped [33, 34]. Therefore, if taking advantage of the anti-sunward surface of a solar absorber panel
34
35 by covering it with a layer of radiative cooling material, and rolling over the panel in some way when
36
37 cooling is needed, we can realize PT and RC flexibly in a single collector without diminishing the PT
38
39 or RC capacity. Such dual-nature enables the collector to efficiently carry out either solar heating or
40
41 radiative cooling in line with dynamic energy demands. In the present study, we designed and
42
43 manufactured such a rotatable photothermic and radiative cooling (PT-RC) collector. Furthermore, we
44
45 deployed an outdoor PT-RC testing rig to quantitatively characterize the thermal performance of the
46
47 rotatable PT-RC system in solar heating and radiative cooling modes.
48
49
50
51
52
53
54
55
56
57
58

59 **2. Rotatable PT-RC system**

60
61
62
63
64
65

1 The rotatable PT-RC collector is arranged as a flat-plate structure which mainly includes a
2
3 transparent cover, a rotatable PT-RC panel, ten groups of branch copper tubes, two manifold copper
4
5 tubes, and a stretchable thermal insulation layer, and several frames. Fig. 1 illustrates the cross-section
6
7 view of the rotatable PT-RC collector. A 6 μm -thick polyethylene (PE) film is employed as the
8
9 transparent cover of the collector to suppress convective heat exchange between the panel and ambient
10
11 air. The rotatable PT-RC panel, consisted of ten strips of sub-PT-RC panels, is coated with a solar
12
13 selected absorbing coating on one surface while a radiative cooling layer (provided by Ningbo Radi-
14
15 Cool Advanced Energy Technologies Co., Ltd) on the opposite surface. The spectral properties of the
16
17 two surfaces, namely, the solar absorber (PT side) and the radiative emitter (RC side), are shown in
18
19 Fig. 2. The solar absorber shows a high absorptivity in the solar spectrum and a low emissivity in the
20
21 rest bands, indicating an excellent solar thermal performance. In contrast, the radiative emitter presents
22
23 a low solar absorptivity and a high thermal emissivity, suggesting a good radiative cooling capacity.
24
25 Ten groups of concentric copper tubes, with the outer tubes being welded on the RC side of the panel
26
27 and the inner ones being connected with the two manifold copper tubes evenly, are acted as the heat
28
29 conductor. The internal diameter of the outer tube is only slightly greater than the external diameter of
30
31 the inner tube. This design enables the PT-RC panel, together with the outer tubes, to rotate freely
32
33 around the inner tubes and effectively transfer heat or coldness to the water flow passed through the
34
35 inner tube. The rotation is manual in this proof-of-concept study. However, in real-world applications,
36
37 automatic or gearing schemes can be involved to achieve more advanced rotation. With a thickness of
38
39 50 mm and thermal conductivity of $0.046 \text{ W}/(\text{m}^2 \cdot \text{K})$, the thermal insulation layer is placed at the
40
41 bottom of the collector to suppress the backward heat loss of the PT-RC panel. A list of some key
42
43 structural and thermophysical parameters of the PT-RC collector is shown in Table 1.
44
45
46
47
48
49
50
51
52
53
54
55
56
57
58
59
60
61
62
63
64
65

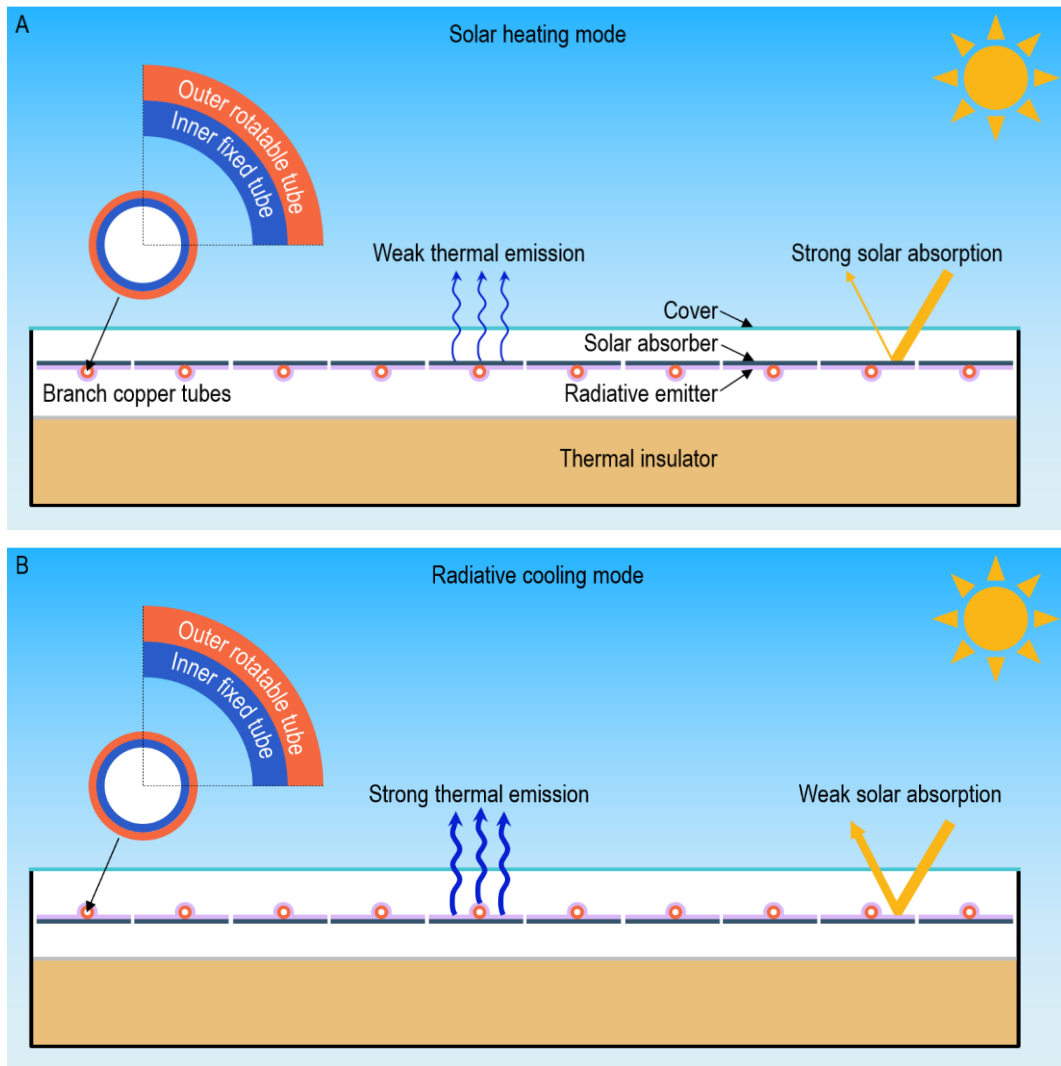


Fig. 1. Cross-section view of the rotatable PT-RC collector working in (A) solar heating mode and (B) radiative cooling mode.

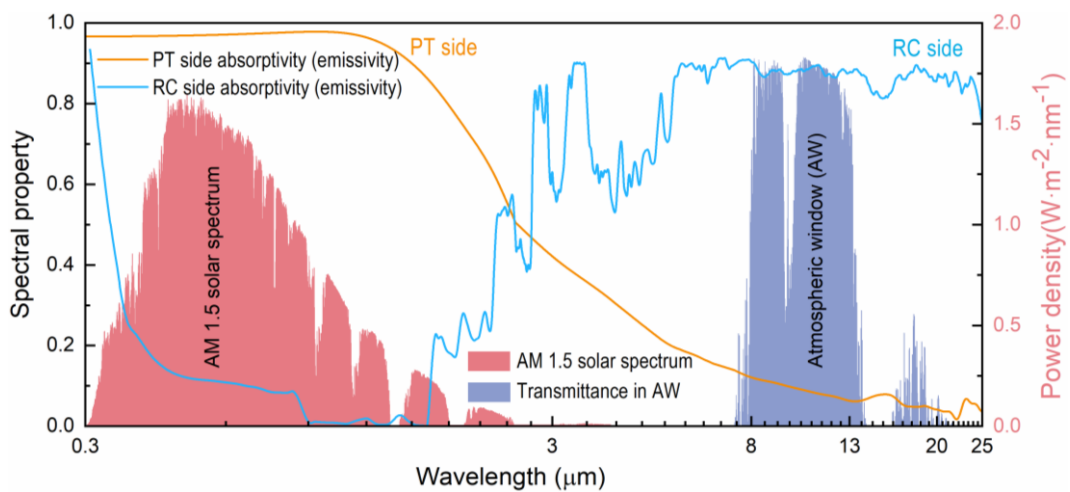


Fig. 2. Spectral properties of the solar absorber (PT side) and radiative emitter (RC side). The curves are smoothed using Origin 2020. The normalized AM 1.5 solar spectrum and typical transmissivity of the atmospheric window are plotted for reference.

Table 1. Some key structural and thermophysical parameters of the PT-RC collector.

Components	Parameters	Values
Cover (PE film)	Length (m)	1.95
	Width (m)	0.96
	Thickness (μm)	6
PT-RC panel (aluminum sheet as substrate)	Solar absorptivity (PT side)	0.951
	Solar absorptivity (RC side)	0.135
	Thermal emissivity (PT side)	0.088
	Thermal emissivity (RC side)	0.927
	Thickness (mm)	0.6
Branch copper tube	External diameter of inner tubes (m)	0.01
	Internal diameter of inner tubes (m)	0.008
	External diameter of outer tubes (m)	0.013
	Internal diameter of outer tubes (m)	0.011
	Number	20
Manifold copper tube	Center distance between groups (m)	0.096
	External diameter (m)	0.02
	Internal diameter (m)	0.018
Backside thermal insulation	Number	2
	Thermal conductivity ($\text{W}\cdot\text{m}^{-1}\cdot\text{K}^{-1}$)	0.046
Air gap between the cover and panel	Thickness (m)	0.05
	Height (m)	0.04

As shown in Figs. 3 and 4, the rotatable PT-RC system is formed by connecting the PT-RC collector with a 120 L circulation water tank using two thermal-insulated water pipes. The water tank act as a hot storage tank in solar heating mode and a cold storage tank in radiative cooling mode. In real-world applications, however, it may be better to arrange two separate water tanks for the system to store heat and coldness, respectively. The water flow circulates continuously in the closed water loop during each test. Thus, the water temperature in the tank can be gradually heated up in solar heating mode or cooled down in radiative cooling mode. The PT-RC collector is placed due south on iron support with an inclination angle of 32° which is equal to the local (Hefei, China) latitude. A water pump, a water flowmeter, and a valve are arranged on the water pipe. Two platinum resistors are respectively installed at the inlet and outlet of the PT-RC collector to measure the inlet and outlet water

1 temperatures. Five thermocouples are connected with the PT-RC panel along the water flow direction
 2 to monitor the panel temperature. Another five thermocouples are inserted in the water tank evenly
 3 along the height to measure the average water temperature. One more thermocouple is placed in a
 4 nearby thermometer shelter to record the ambient temperature. A pyranometer is installed on the iron
 5 support with the same inclination angle to measure solar irradiance. An anemometer is set nearby to
 6 monitor the ambient wind velocity. All measured data were recorded by a data logger every 10 seconds.
 7
 8 Testing and monitoring devices involved in the PT-RC experimental system and their uncertainties are
 9 listed in Table 2.
 10
 11
 12
 13
 14
 15
 16
 17
 18
 19
 20
 21
 22
 23
 24
 25
 26
 27
 28
 29
 30
 31
 32
 33
 34
 35
 36
 37
 38
 39
 40
 41
 42
 43
 44
 45
 46
 47
 48
 49
 50
 51
 52
 53
 54
 55
 56
 57
 58
 59
 60
 61
 62
 63
 64
 65

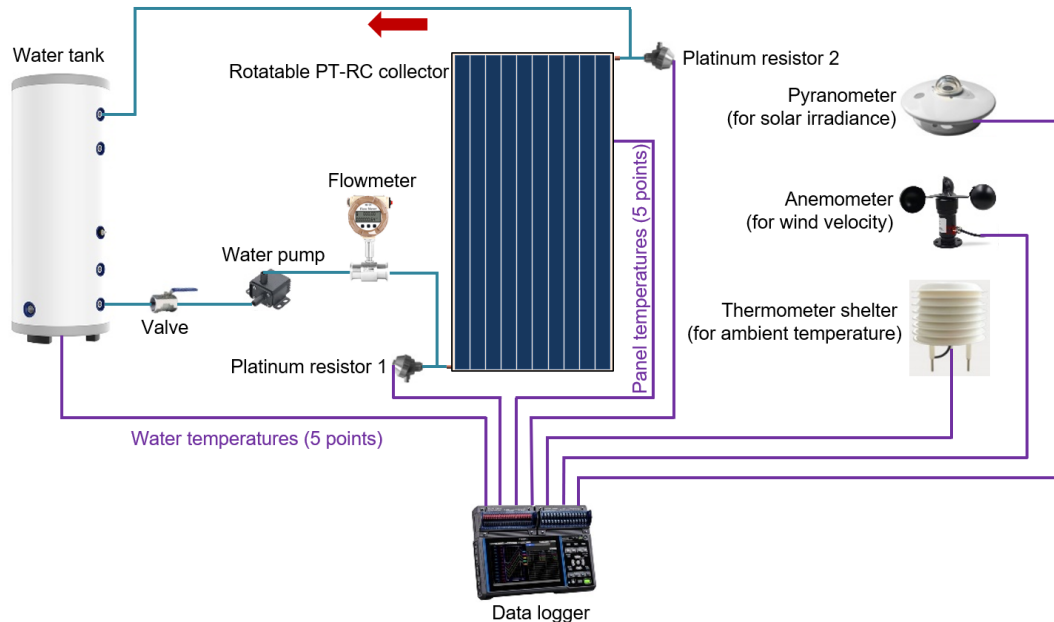


Fig. 3. Schematic of the rotatable PT-RC experimental system.

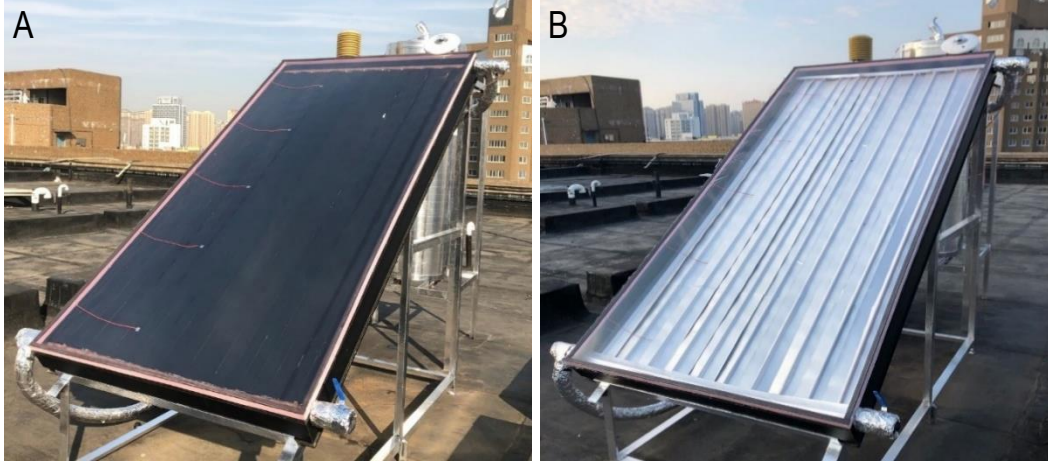


Fig. 4. In-situ experimental setup of the rotatable PT-RC system working in (A) solar heating mode and (B) radiative cooling mode. The experimental system is located on the rooftop of a building in the University of Science and Technology of China, Hefei, China.

Table 2. List of testing and monitoring devices in the rotatable PT-RC experimental system.

Device	Specification	Uncertainty
Pyranometer	TBQ-2A	$\pm 2\%$
Anemometer	HSTL-FS01	± 0.2 m/s
Water flowmeter	LWGY-C	$\pm 0.5\%$
Thermocouple	Type T	± 0.5 °C
Platinum resistor	OMEGA-PT100	$\pm (0.03+0.001 t)$ °C
Data logger	HIOKI LR8450	/

3. Performance indicators

Attributed to the rotatable structure, the PT-RC system can operate in either solar heating or radiative cooling modes in line with weather conditions and energy demands.

In solar heating mode, the daily average thermal efficiency of the rotatable PT-RC system is set as the performance indicator, which is the total heat gain of water in the water tank divided by the total incident solar energy during the test, expressed as:

$$\eta_{th} = \frac{Q_{total}}{GA_c} = \frac{Mc_w (T_{w_end} - T_{w_start})}{GA_c} \quad (1)$$

where Q_{total} signifies the total heat gain of water in the water tank during the test, J; G is the total

1 incident solar energy per square meter, J/m^2 ; A_c is aperture area of the PT-RC collector, m^2 ; M is the
2
3 mass of water in the water tank, kg; c_w is the specific heat capacity of water, $J/(kg \cdot K)$; and T_{w_start} and
4
5
6 T_{w_end} are correspondingly the water temperature in the tank at the start and end of the test, K.
7

8
9 In radiative cooling mode, the instantaneous cooling power of the PT-RC collector and the total
10
11 cooling energy gain of the PT-RC system are set as two performance indicators.
12

13
14 The instantaneous cooling power of the PT-RC collector is defined as the dissipated heat of the
15
16 water flow passing through the collector, expressed as:
17

$$18 \quad P_{cooling} = \frac{\dot{m}c_w (T_{w_in} - T_{w_out})}{A_c} \quad (2)$$

19
20 where \dot{m} is the mass flow rate of the water flow, kg/s; and T_{w_in} and T_{w_out} are respectively the water
21
22 temperature at the inlet and outlet of the collector, K.
23

24
25 The total cooling energy gain of the PT-RC system is the total cooling energy gain of water in the
26
27 tank during the test, expressed as:
28

$$29 \quad Q_{cooling} = Mc_w (T_{w_start} - T_{w_end}) \quad (3)$$

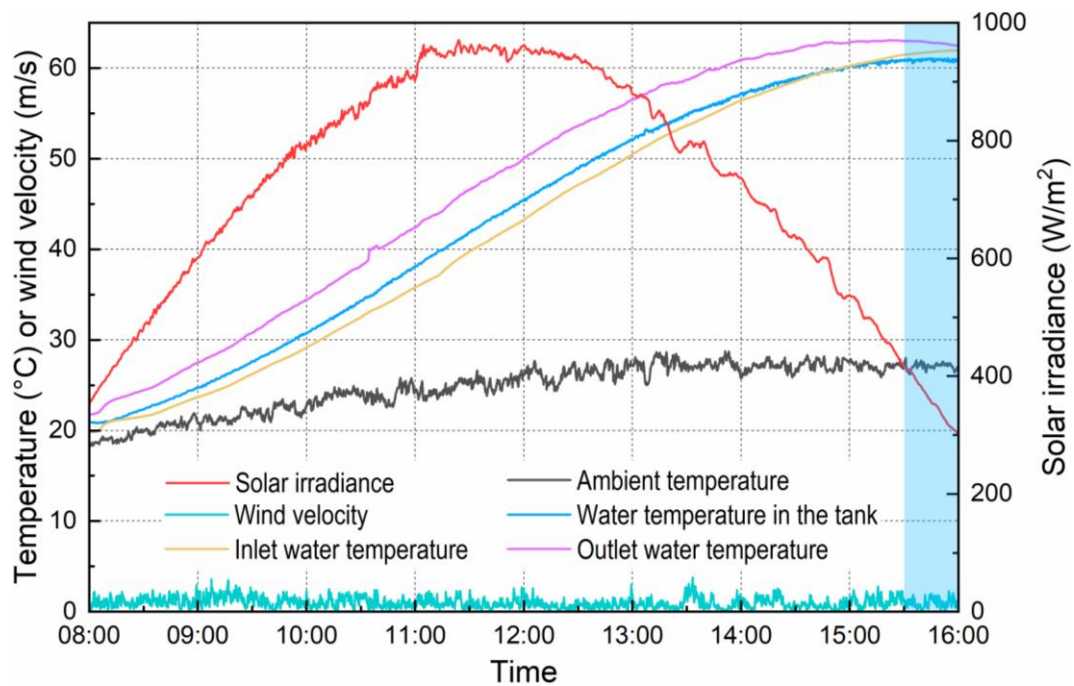
30 31 32 33 34 35 36 37 38 39 **4. Results and discussion**

40 41 42 *4.1. Solar heating mode*

43 44 45 *4.1.1. Single-day solar heating test*

46
47 Firstly, the rotatable PT-RC system running in solar heating mode was measured. Fig. 5 presents
48
49 the weather data on a typical day and the water temperature variations in the water tank and at the inlet
50
51 and outlet of the PT-RC collector during the test. The sum of incident solar energy was 39.4 MJ, and
52
53 the average ambient temperature was 24.8 °C. The initial water temperature in the water tank (21.0 °C)
54
55 was only slightly higher than the ambient temperature (18.6 °C). As time went on, the temperature gap
56
57
58
59
60
61
62
63
64
65

1 between the water and ambient air enlarged, with the water temperature ending at 60.8 °C, which is
 2
 3 34.2 °C higher than the ambient temperature. The water temperature plateaued or even slightly
 4
 5
 6 decreased during the last half-hour of the test (bluish area), attributed to the weak and sharply declined
 7
 8
 9 solar intensity and large thermal loss of the system. Unlike a solar photovoltaic/thermal system which
 10
 11 can still generate electricity even though the solar radiation is poor, it is recommended to stop the
 12
 13 operation of the rotatable PT-RC system earlier to save pump power consumption. In real-world
 14
 15 applications, the pump in most solar water heating systems can be turned on/off automatically
 16
 17 depending on inlet-out let temperature difference of the collector field, storage tank, etc. The thermal
 18
 19 efficiency of the system during the test was recorded at 51.6% and could increase to 53.3% if the
 20
 21 system was shut down at 15:30.
 22
 23
 24
 25
 26



27
 28
 29
 30
 31
 32
 33
 34
 35
 36
 37
 38
 39
 40
 41
 42
 43
 44
 45
 46
 47
 48
 49
 50
 51
 52 Fig. 5. Weather data and water temperature profile of the rotatable PT-RC system on October 20th, 2019 in Hefei,
 53
 54
 55
 56
 57
 58
 59
 60
 61
 62
 63
 64
 65
 66
 67
 68
 69
 70
 71
 72
 73
 74
 75
 76
 77
 78
 79
 80
 81
 82
 83
 84
 85
 86
 87
 88
 89
 90
 91
 92
 93
 94
 95
 96
 97
 98
 99
 100
 101
 102
 103
 104
 105
 106
 107
 108
 109
 110
 111
 112
 113
 114
 115
 116
 117
 118
 119
 120
 121
 122
 123
 124
 125
 126
 127
 128
 129
 130
 131
 132
 133
 134
 135
 136
 137
 138
 139
 140
 141
 142
 143
 144
 145
 146
 147
 148
 149
 150
 151
 152
 153
 154
 155
 156
 157
 158
 159
 160
 161
 162
 163
 164
 165
 166
 167
 168
 169
 170
 171
 172
 173
 174
 175
 176
 177
 178
 179
 180
 181
 182
 183
 184
 185
 186
 187
 188
 189
 190
 191
 192
 193
 194
 195
 196
 197
 198
 199
 200
 201
 202
 203
 204
 205
 206
 207
 208
 209
 210
 211
 212
 213
 214
 215
 216
 217
 218
 219
 220
 221
 222
 223
 224
 225
 226
 227
 228
 229
 230
 231
 232
 233
 234
 235
 236
 237
 238
 239
 240
 241
 242
 243
 244
 245
 246
 247
 248
 249
 250
 251
 252
 253
 254
 255
 256
 257
 258
 259
 260
 261
 262
 263
 264
 265
 266
 267
 268
 269
 270
 271
 272
 273
 274
 275
 276
 277
 278
 279
 280
 281
 282
 283
 284
 285
 286
 287
 288
 289
 290
 291
 292
 293
 294
 295
 296
 297
 298
 299
 300
 301
 302
 303
 304
 305
 306
 307
 308
 309
 310
 311
 312
 313
 314
 315
 316
 317
 318
 319
 320
 321
 322
 323
 324
 325
 326
 327
 328
 329
 330
 331
 332
 333
 334
 335
 336
 337
 338
 339
 340
 341
 342
 343
 344
 345
 346
 347
 348
 349
 350
 351
 352
 353
 354
 355
 356
 357
 358
 359
 360
 361
 362
 363
 364
 365
 366
 367
 368
 369
 370
 371
 372
 373
 374
 375
 376
 377
 378
 379
 380
 381
 382
 383
 384
 385
 386
 387
 388
 389
 390
 391
 392
 393
 394
 395
 396
 397
 398
 399
 400
 401
 402
 403
 404
 405
 406
 407
 408
 409
 410
 411
 412
 413
 414
 415
 416
 417
 418
 419
 420
 421
 422
 423
 424
 425
 426
 427
 428
 429
 430
 431
 432
 433
 434
 435
 436
 437
 438
 439
 440
 441
 442
 443
 444
 445
 446
 447
 448
 449
 450
 451
 452
 453
 454
 455
 456
 457
 458
 459
 460
 461
 462
 463
 464
 465
 466
 467
 468
 469
 470
 471
 472
 473
 474
 475
 476
 477
 478
 479
 480
 481
 482
 483
 484
 485
 486
 487
 488
 489
 490
 491
 492
 493
 494
 495
 496
 497
 498
 499
 500
 501
 502
 503
 504
 505
 506
 507
 508
 509
 510
 511
 512
 513
 514
 515
 516
 517
 518
 519
 520
 521
 522
 523
 524
 525
 526
 527
 528
 529
 530
 531
 532
 533
 534
 535
 536
 537
 538
 539
 540
 541
 542
 543
 544
 545
 546
 547
 548
 549
 550
 551
 552
 553
 554
 555
 556
 557
 558
 559
 560
 561
 562
 563
 564
 565
 566
 567
 568
 569
 570
 571
 572
 573
 574
 575
 576
 577
 578
 579
 580
 581
 582
 583
 584
 585
 586
 587
 588
 589
 590
 591
 592
 593
 594
 595
 596
 597
 598
 599
 600
 601
 602
 603
 604
 605
 606
 607
 608
 609
 610
 611
 612
 613
 614
 615
 616
 617
 618
 619
 620
 621
 622
 623
 624
 625
 626
 627
 628
 629
 630
 631
 632
 633
 634
 635
 636
 637
 638
 639
 640
 641
 642
 643
 644
 645
 646
 647
 648
 649
 650
 651
 652
 653
 654
 655
 656
 657
 658
 659
 660
 661
 662
 663
 664
 665
 666
 667
 668
 669
 670
 671
 672
 673
 674
 675
 676
 677
 678
 679
 680
 681
 682
 683
 684
 685
 686
 687
 688
 689
 690
 691
 692
 693
 694
 695
 696
 697
 698
 699
 700
 701
 702
 703
 704
 705
 706
 707
 708
 709
 710
 711
 712
 713
 714
 715
 716
 717
 718
 719
 720
 721
 722
 723
 724
 725
 726
 727
 728
 729
 730
 731
 732
 733
 734
 735
 736
 737
 738
 739
 740
 741
 742
 743
 744
 745
 746
 747
 748
 749
 750
 751
 752
 753
 754
 755
 756
 757
 758
 759
 760
 761
 762
 763
 764
 765
 766
 767
 768
 769
 770
 771
 772
 773
 774
 775
 776
 777
 778
 779
 780
 781
 782
 783
 784
 785
 786
 787
 788
 789
 790
 791
 792
 793
 794
 795
 796
 797
 798
 799
 800
 801
 802
 803
 804
 805
 806
 807
 808
 809
 810
 811
 812
 813
 814
 815
 816
 817
 818
 819
 820
 821
 822
 823
 824
 825
 826
 827
 828
 829
 830
 831
 832
 833
 834
 835
 836
 837
 838
 839
 840
 841
 842
 843
 844
 845
 846
 847
 848
 849
 850
 851
 852
 853
 854
 855
 856
 857
 858
 859
 860
 861
 862
 863
 864
 865
 866
 867
 868
 869
 870
 871
 872
 873
 874
 875
 876
 877
 878
 879
 880
 881
 882
 883
 884
 885
 886
 887
 888
 889
 890
 891
 892
 893
 894
 895
 896
 897
 898
 899
 900
 901
 902
 903
 904
 905
 906
 907
 908
 909
 910
 911
 912
 913
 914
 915
 916
 917
 918
 919
 920
 921
 922
 923
 924
 925
 926
 927
 928
 929
 930
 931
 932
 933
 934
 935
 936
 937
 938
 939
 940
 941
 942
 943
 944
 945
 946
 947
 948
 949
 950
 951
 952
 953
 954
 955
 956
 957
 958
 959
 960
 961
 962
 963
 964
 965
 966
 967
 968
 969
 970
 971
 972
 973
 974
 975
 976
 977
 978
 979
 980
 981
 982
 983
 984
 985
 986
 987
 988
 989
 990
 991
 992
 993
 994
 995
 996
 997
 998
 999
 1000

4.1.2. Multi-day solar heating test

1 As the weather condition and initial temperature difference between the water in the tank and
 2 ambient air will influence the thermal performance of a solar thermal system, we conducted multi-day
 3 testing on several sunny or mostly sunny days to eliminate this influence and reveal the thermal
 4 efficiency of the rotatable PT-RC system at different reduced temperatures $(T_{w_start} - \bar{T}_a)/H'$, which is
 5 a more rigorous performance indicator for a solar thermal system. T_{w_start} and \bar{T}_a are respectively the
 6 initial water temperature in the tank and the average ambient temperature during the test, K; and H' is
 7 the total incident solar energy per square meter, MJ/m².

8 The test period on each testing day was 8:00 to 16:00. The thermal efficiency of the system at
 9 different reduced temperatures is plotted in Fig. 6, with more detailed experimental data presented in
 10 Table 3. According to the fitting curve in Fig. 6, the linear regression equation for thermal efficiency
 11 can be expressed as Eq. (4), in which 50.4% is the thermal efficiency of the rotatable PT-RC system at
 12 zero-reduced temperature (when the initial water temperature in the water tank equals the average
 13 ambient temperature during the test, i.e., $(T_{w_start} - \bar{T}_a)/H' = 0$); and 0.125 is the heat loss coefficient
 14 of the system. With a thermal efficiency of over 50% at zero-reduced temperature, we can conclude
 15 that, though the spectral property of the cover material (PE film) is different from the glass cover in
 16 typical solar collectors, the thermal performance of the rotatable PT-RC system is comparable to that
 17 of typical flat-plate solar water heating systems [29, 35] and much higher than that of the spectrally-
 18 coupled PT-RC system (38.6%) in our previous work [29].

$$\bar{\eta}_{th} = 0.504 - 0.125 \frac{T_{w_start} - \bar{T}_a}{H'} \quad (4)$$

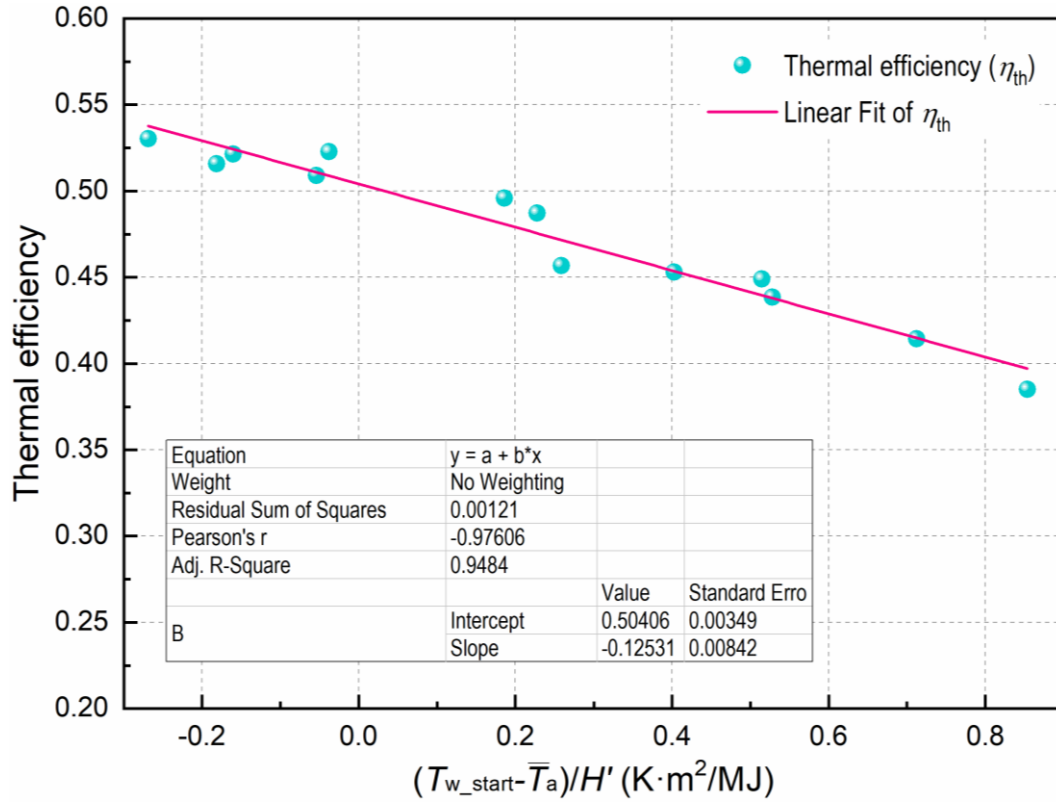


Fig. 6. The thermal efficiency of the PT-RC system at different reduced temperatures in a multi-day solar heating test.

Table 3. Multi-day solar heating testing results (data from 08:00 to 16:00).

Day No.	H (MJ)	\bar{T}_a (°C)	T_{w_start} (°C)	T_{w_end} (°C)	$(T_{w_start} - \bar{T}_a)/H'$ (K·m²/MJ)	ΔT_w (°C)	η_{th} (%)
1	39.4	24.8	21.0	60.8	-0.181	39.8	51.6
2	35.0	24.7	29.5	60.8	0.259	31.3	45.7
3	31.9	23.0	26.8	57.2	0.228	30.4	48.7
4	30.5	24.1	23.5	54.8	-0.0377	31.3	52.3
5	33.3	20.6	23.9	56.2	0.186	32.3	49.6
6	32.8	22.5	31.4	60.3	0.515	28.9	44.9
7	36.1	23.6	20.5	57.4	-0.160	36.9	52.1
8	36.2	24.8	32.5	64.7	0.403	32.2	45.3
9	29.9	24.9	20.7	51.7	-0.269	31.0	53.0
10	24.1	22.6	31.7	51.3	0.712	19.6	41.4
11	32.1	23.2	32.1	59.7	0.528	27.6	43.8
12	28.0	20.5	33.1	54.2	0.854	21.1	38.5
13	32.0	19.8	18.8	50.8	-0.0540	32.0	50.9

4.2. Radiative cooling mode

4.2.1. Consecutive 32-hour radiative cooling test

1 By rotating the PT-RC panel with the RC side facing the sky, the cooling performance of the
2
3 rotatable PT-RC system was measured in a consecutive 32-hour period, during which the sky was very
4
5 clear both in daytime and nighttime. Experimental results revealed that the PT-RC collector could not
6
7 achieve radiative cooling in most daytime hours, evidenced by the gradually increasing water
8
9 temperature in the water tank (see Fig. 7A). The deactivation of daytime radiative cooling is mainly
10
11 attributed to the limited solar reflectivity of the radiative emitter. As shown in Table 1, the solar
12
13 reflectivity of the radiative emitter is 0.865, which is much lower than the radiative emitter with a
14
15 similar structure but a solar reflectivity of 0.95 [36]. The climate and geographical conditions in Hefei
16
17 are also responsible for the failure of achieving daytime radiative cooling in this study. In Boulder with
18
19 an arid climate and an altitude of over 1600 m, the radiative emitter realized an average cooling power
20
21 of 45 W/m² under an average solar irradiance of 952 W/m² at noon (12:00 to 14:00) [36]. However, in
22
23 Hefei with a humid climate and an altitude of only 30 m, the radiative emitter could not achieve sub-
24
25 ambient cooling and showed an average heating power of 68 W/m² under 807 W/m² average solar
26
27 irradiance during the same period. Our long-term testing further demonstrated that the rotatable PT-
28
29 RC system at Hefei generally could not realize daytime radiative cooling no matter on sunny, cloudy,
30
31 or overcast days. Although the solar intensity was lower when the sky was cloudy or overcast, the
32
33 atmospheric transmittance was also much lower. In this case, the absorbed solar heat still exceeded the
34
35 dissipated radiative heat. However, the fact that the present rotatable PT-RC collector cannot achieve
36
37 daytime sub-ambient radiative cooling does not signify that it is meaningless operating as a daytime
38
39 radiative cooler. Regardless of the potential that it might provide all-day coldness in certain locations
40
41 with RC-friendly ambient conditions, its possible contribution in cutting down energy consumption is
42
43 worth pointing out. For example, even though the building envelop is well-insulated, its external
44
45
46
47
48
49
50
51
52
53
54
55
56
57
58
59
60
61
62
63
64
65

1 surface will be heated up to a high temperature due to the high solar absorptivity, and thus a non-
2 negligible amount of heat will be gradually transferred into the room through the insulation structure
3 inevitably. However, installing the PT-RC collector onto the building roof or façade and switching its
4 working mode to radiative cooling in hot seasons can reduce the cooling load of the building since
5 most of the solar energy that the building envelope would otherwise absorb will be rejected by the PT-
6 RC collector. Furthermore, the rotatable PT-RC system could easily achieve radiative cooling at night,
7 early morning, and late afternoon when the solar irradiance is zero or very low. As shown in Fig. 7A,
8 the water temperature in the water tank, with an initial temperature of 17.4 °C, decreased slightly in
9 the first half an hour when the solar radiation was weak and then increased to 23.8 °C around 16:10
10 on Nov 17th, 2020 when the solar irradiance was 215.8 W/m². After that, the water declined gradually
11 to a minimum temperature of 14.3 °C around 07:25 on Nov 18th, 2020 when the solar irradiance was
12 166.3 W/m². Then, the water temperature remained relatively stable before increasing again from
13 around 08:30 to 16:00, with an ending value of 21.5 °C.

14 The instantaneously cooling power, regardless of the heat exchange occurring in the water tank
15 and connecting water pipes, characterizes the cooling performance of the rotatable PT-RC collector
16 rather than the whole system. As shown in Fig. 7B, the cooling power value was negative during most
17 daytime hours, indicating that the water was heated up when passing through the collector. Generally,
18 the heating power during the daytime was almost equivalent to the cooling power during the nighttime.
19 The profile of the cooling power was exactly the opposite of that of the solar irradiance, except that
20 the value plateaued in general during peak solar hours. This abnormal phenomenon can be traced to
21 the structural design of the rotatable PT-RC panel. As presented in Figs. 3 and 4, there exist tiny gaps
22 between adjacent sub-PT-RC panels, allowing a fraction of solar radiation, both direct and diffuse parts,

1 to pass through and finally be absorbed by the PT side of the panel. When the incident angle of direct
2
3 solar radiation is large, namely, in the early morning and late afternoon, these tiny gaps are more likely
4
5 to capture direct solar radiation and guide it to the PT side of the panel. However, when the incident
6
7 angle of direct solar radiation is limited within a small level, namely, around noon, less proportion of
8
9 direct solar radiation will be finally absorbed by the PT side. In conclusion, a lower incident angle of
10
11 direct solar radiation signifies greater solar energy absorption by the RC side but less by the PT side,
12
13 resulting in relatively stable negative cooling power (i.e., heating power) during peak solar hours. This
14
15 enlightens the importance of optimizing the gap structure to eliminate unwanted solar absorption and
16
17 improve daytime radiative cooling performance in future studies.
18
19
20
21
22
23
24

25 The PT-RC collector could output net cooling energy from 15:50 to 07:50, during which the
26
27 adverse impact of solar radiation was overwhelmed by the thermal emission of the collector itself. In
28
29 particular, the collector operated in quasi-steady-state from 17:00 to 07:00, with the cooling power
30
31 slightly decreasing from roughly 60 to 50 W/m². This gradual decline is in line with the principle
32
33 revealed by the well-known Planck's law. That is, with the water temperature being cooled down by
34
35 radiative cooling, the panel temperature gradually decreased from approximately 20 to 12 °C, and thus
36
37 the outward radiative power of the panel experienced a slow reduction during this period.
38
39 Paradoxically, on the one hand, we prefer to deliver colder working medium (e.g., cold water and air)
40
41 for end-users; on the other hand, the cooling performance of a radiative cooling system will deteriorate
42
43 at lower temperatures.
44
45
46
47
48
49
50
51
52
53
54
55
56
57
58
59
60
61
62
63
64
65

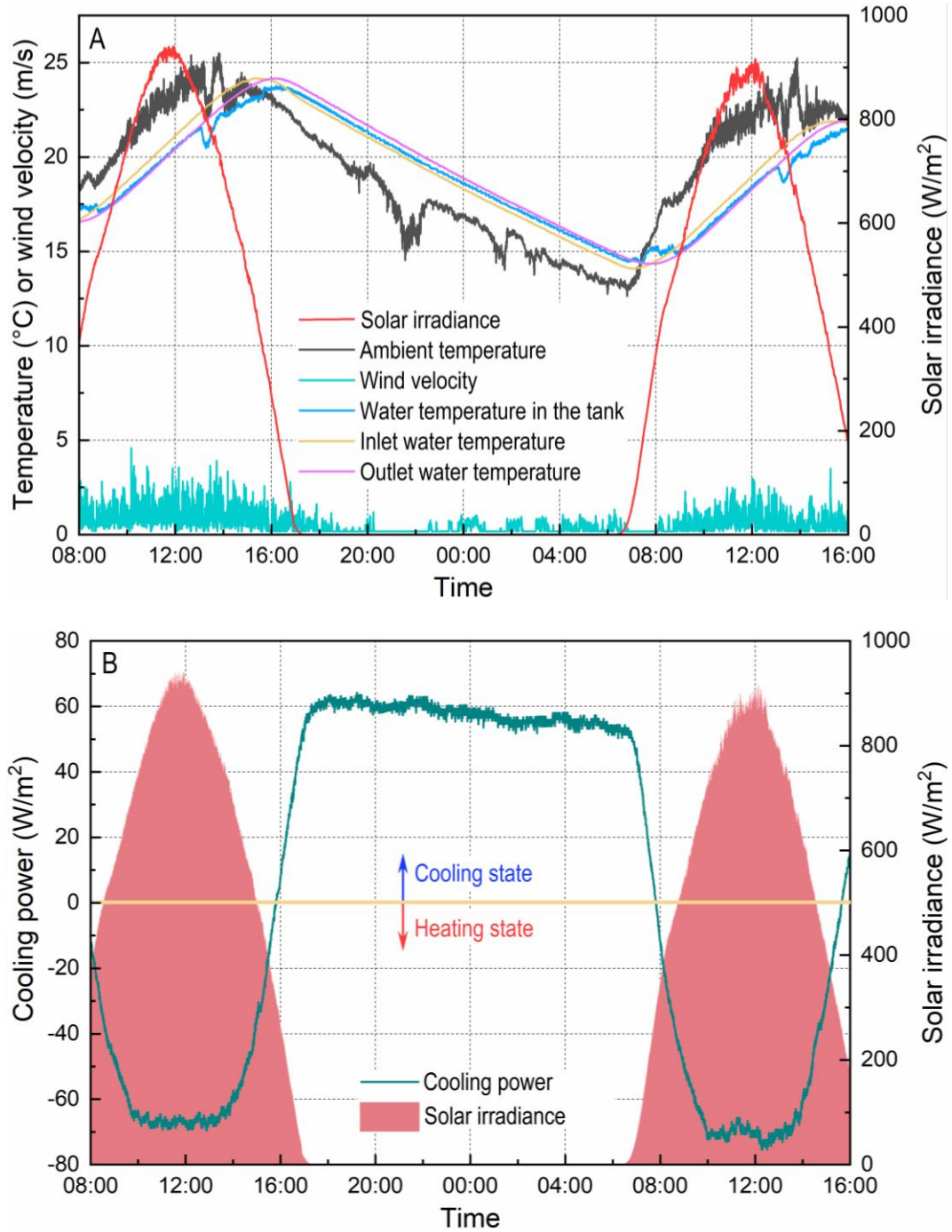


Fig. 7. Weather data and cooling performance of the rotatable PT-RC system on November 7th and 8th, 2020 in Hefei, China.

4.2.2. Multi-night radiative cooling test

Considering that the PT-RC system had proved unable to realize daytime sub-ambient radiative cooling in Hefei, we focused on testing its nocturnal cooling performance. As the weather condition,

in particular, the sky transmittance, dominates the performance of a radiative cooling-driven system, we investigated the nighttime cooling behaviour of the PT-RC system on several nights. As shown in Table 4, the cooling performance of the system varied distinctly among selected nights. The water temperature-reduction in the water tank (ΔT_w) could reach 8.3 °C over the clearest night (from 18:00 to 07:00), but reduced by more than half over the most overcast night. Correspondingly, the cooling energy gain (Q_{cooling}) throughout the night changed between 1.9 and 4.2 MJ. The average cooling power of the PT-RC collector (\bar{P}_{cooling}) is a more appropriate indicator to reveal the effect of weather conditions and to compare the radiative cooling performance on different nights. This value ranged from 30.5 to 57.5 W/m² among different nights, which is comparable to several other radiative cooling systems we tested in Hefei [29, 37, 38], but is significantly less than that recorded in Boulder at night (around 80 W/m² on average) [36], further indicating that climate and geographic conditions are critical factors in determining radiative cooling performance. Therefore, it is unfair and unobjective to judge and compare the radiative cooling capacity of different radiative cooling materials or systems applied in different regions without taking into account the difference in weather conditions (e.g., solar intensity, relative humidity, altitude). Besides, no regression equation for the cooling power of the rotatable PT-RC system can be derived from the multi-night radiative cooling testing results, unlike that for the daytime solar thermal efficiency presented in Eq. (4) and Fig. 6.

Table 4. Multi-night radiative cooling testing results (data from 18:00 to 07:00).

Night No.	\bar{T}_a (°C)	T_{w_start} (°C)	T_{w_end} (°C)	ΔT_w (°C)	Q_{cooling} (MJ)	\bar{P}_{cooling} (W/m ²)	$P_{\text{cooling_max}}$ (W/m ²)
1	16.7	19.9	15.7	4.2	2.1	31.7	39.5
2	17.0	21.9	17.1	4.8	2.4	31.8	46.8
3	15.6	22.5	14.2	8.3	4.2	55.6	61.4
4	15.0	19.7	16.0	3.7	1.9	30.5	62.2
5	17.5	22.9	16.8	6.1	3.1	46.2	55.1
6	16.3	22.7	14.6	8.1	4.1	57.5	64.2
7	15.4	20.8	13.8	7.0	3.5	51.1	54.0
8	14.3	19.6	12.8	6.8	3.4	50.1	50.9

9	14.8	19.3	12.7	6.6	3.3	50.1	54.8
10	14.8	19.8	13.3	6.5	3.3	49.5	50.5
11	15.0	20.4	13.9	6.5	3.3	49.2	52.7

4.3. Uncertainty analysis

Considering the limited accuracy of the measuring instruments and the variation of meteorological parameters, the uncertainty of the experimental result needs to be evaluated. The root sum-of-the-squares method is applied to conduct the uncertainty analysis, with the evaluating formula being [39]:

$$U_f = \sqrt{\sum_{i=1}^n \left(\frac{\partial f}{\partial x_i} \right)^2 (\Delta x_i)^2} \quad (5)$$

Based on Eq. (5), the maximum uncertainty values of the performance indicators of the PT-RC system are calculated. In solar heating mode, the maximum uncertainty of thermal efficiency (η_{th}) is $\pm 3.40\%$. In radiative cooling mode, the maximum uncertainties of $P_{cooling}$ and $Q_{cooling}$ are $\pm 7.08 \text{ W/m}^2$ and $\pm 0.357 \text{ MJ}$, respectively.

5. Conclusions

In the present work, a rotatable solar photothermic and radiative cooling (PT-RC) system is proposed, designed, fabricated, and experimentally investigated. The novel PT-RC system, featuring a rotatable PT-RC panel, can operate in either solar heating or radiative cooling modes in tune with the specific energy demand. The daily solar thermal efficiency of the PT-RC system hit 51.6% on a typical sunny day from 8:00 to 16:00, but the heat gain after 15:30 was negligible due to weak solar intensity and significant heat loss. A multi-day solar heating test revealed that, originated from data regression, the daily thermal efficiency of the system at zero-reduced temperature reached 50.4%, which is comparable to that of the common flat-plate solar water heating system and significantly greater than that of the reported spectrally-coupled PT-RC system. A continuous 32-hour radiative cooling test

1 demonstrated that the rotatable PT-RC system could not generate a sub-ambient cooling effect in most
2
3 daytime scenarios in Hefei due to large solar absorption and adverse ambient conditions, but could
4
5 easily output cooling energy at night, early morning and late afternoon. The rotatable PT-RC collector
6
7 itself could provide a gradually declined cooling power from roughly 60 to 50 W/m² as the circulated
8
9 water being continuously cooled down from 20 to 12 °C approximately. The average nocturnal cooling
10
11 power of the PT-RC collector varied from 30.5 to 57.5 W/m² in a multi-night radiative cooling test,
12
13 which is much less than that of a similar radiative cooling system located at a more RC-friendly
14
15 location. This finding suggests that it is unnecessary and pointless to compare the radiative cooling
16
17 capacity of different radiative emitters or systems in different regions with different climate and
18
19 geographical conditions. As heating and cooling are increasingly essential in modern society
20
21 challenged by the energy crisis, this work brings out a new vision for flexibly providing heat and
22
23 coldness in a renewable and environmental-friendly manner, and can possibly be extended to energy-
24
25 saving applications in buildings, vehicles, agriculture, etc. For instance, by integrating the rotatable
26
27 PT-RC collector with the building envelope properly, it can either work as a stand-alone unit for space
28
29 heating/cooling directly or couple with an inherent Heating, Ventilation and Air Conditioning (HVAC)
30
31 system to decrease the heating/cooling loads, which could be the focus of future research.
32
33
34
35
36
37
38
39
40
41
42
43
44

45 **Acknowledgments**

46
47 This study was sponsored by the H2020 Marie Skłodowska-Curie Actions - Individual Fellowships
48
49 (842096), National Natural Science Foundation of China (NSFC 51906241 and 51776193), and Anhui
50
51 Provincial Natural Science Foundation (1908085ME138). We thank Ningbo Radi-Cool Advanced
52
53 Energy Technologies Co., Ltd (<http://www.rl-cool.com>), for providing the radiative cooling metafilm.
54
55
56
57
58

59 **Nomenclature**

60
61
62
63
64
65

1	A	Area, m ²
2	c	Specific heat capacity, J/(kg·K)
3	G	Total incident solar energy, J/m ²
4	H'	Total incident solar energy, MJ/m ²
5	H	Total incident solar energy, MJ
6		
7	P	Cooling power, W/m ²
8		
9	\bar{P}	Average cooling power, W/m ²
10		
11	Q	Thermal energy gain, J
12		
13	T	Temperature, °C
14		
15	\bar{T}	Average temperature, °C
16		
17	ΔT	Temperature difference or measurement uncertainty of temperature sensors, °C
18		
19	η	Solar thermal efficiency, -
20		

21 *Abbreviation and subscripts*

22		
23	a	Ambient air
24		
25	c	Collector
26		
27	cooling	Radiative cooling mode
28		
29	end	Ending time of a test
30		
31	in	Collector inlet
32		
33	max	Maximum
34		
35	out	Collector outlet
36		
37	start	Starting time of a test
38		
39	th	Thermal
40		
41	w	Water
42		
43		

44 **Appendix**

45
46 This appendix contains detailed information for uncertainty analysis conducted in Section 4.3. As
47 listed in Eq. (5), the uncertainty analysis is conducted by using the root sum-of-the-squares method:
48

$$U_f = \sqrt{\sum_{i=1}^n \left(\frac{\partial f}{\partial x_i} \right)^2 (\Delta x_i)^2} \quad (\text{A1})$$

55
56 The uncertainties of performance indicators presented in Section 4.3 are derived as follows:
57

58
59 (1) η_{th}
60
61
62
63
64
65

1 According to Eq. (1), the uncertainty of η_{th} is expressed as:

$$U_{\eta_{th}} = \eta_{th} \sqrt{2 \left(\frac{\Delta T}{T_{w_end} - T_{w_start}} \right)^2 + \left(\frac{\Delta G}{G} \right)^2} \quad (A2)$$

2
3
4
5
6
7 (2) $P_{cooling}$

8 According to Eq. (2), the uncertainty of $P_{cooling}$ is written as:

$$U_{P_{cooling}} = P_{cooling} \sqrt{\left(\frac{\Delta T_{w_in}}{T_{w_out} - T_{w_in}} \right)^2 + \left(\frac{\Delta T_{w_out}}{T_{w_out} - T_{w_in}} \right)^2 + \left(\frac{\Delta \dot{m}}{\dot{m}} \right)^2} \quad (A3)$$

9
10
11
12
13
14
15
16
17 (3) $Q_{cooling}$

18 According to Eq. (3), the uncertainty of $Q_{cooling}$ is calculated by:

$$U_{Q_{cooling}} = Q_{cooling} \frac{\sqrt{2} \cdot \Delta T}{T_{w_end} - T_{w_start}} \quad (A4)$$

19
20
21
22
23
24
25
26
27
28 The ΔT , ΔG , and $\Delta \dot{m}$ are respectively the measurement uncertainty of the thermocouple/platinum
29 resistor, pyranometer, and water flowmeter listed in Table 2.
30
31
32
33

34 References

- 35
36 [1] Ghilardi LMP, Castelli AF, Moretti L, Morini M, Martelli E. Co-optimization of multi-energy system operation, district
37 heating/cooling network and thermal comfort management for buildings. *Applied Energy*. 2021;302:117480.
38 [2] Chakraborty D, Alam A, Chaudhuri S, Bařaęaoęlu H, Sulbaran T, Langar S. Scenario-based prediction of climate change
39 impacts on building cooling energy consumption with explainable artificial intelligence. *Applied Energy*. 2021;291:116807.
40 [3] Bachram H. Climate fraud and carbon colonialism: the new trade in greenhouse gases. *Capitalism nature socialism*.
41 2004;15:5-20.
42 [4] Lindzen R. Straight Talk about Climate Change. *Academic Questions*. 2017;30:419-32.
43 [5] Manfroid J, Hutsemékers D, Jehin E. Iron and nickel atoms in cometary atmospheres even far from the Sun. *Nature*.
44 2021;593:372-4.
45 [6] Li W, Fan S. Radiative cooling: harvesting the coldness of the universe. *Opt Photon News*. 2019;30:32-9.
46 [7] Zhou J, Zhao X, Yuan Y, Li J, Yu M, Fan Y. Operational performance of a novel heat pump coupled with mini-channel
47 PV/T and thermal panel in low solar radiation. *Energy and Built Environment*. 2020;1:50-9.
48 [8] Yu B, Li N, Xie H, Ji J. The performance analysis on a novel purification-cleaning trombe wall based on solar thermal
49 sterilization and thermal catalytic principles. *Energy*. 2021;225:120275.
50 [9] Lingayat AB, Chandramohan VP, Raju VRK, Meda V. A review on indirect type solar dryers for agricultural crops – Dryer
51 setup, its performance, energy storage and important highlights. *Applied Energy*. 2020;258:114005.
52 [10] Khatoon S, Kim M-H. Performance analysis of carbon dioxide based combined power cycle for concentrating solar
53 power. *Energy Conversion and Management*. 2020;205:112416.
54
55
56
57
58
59
60
61
62
63
64
65

- 1 [11] Lin K-T, Lin H, Yang T, Jia B. Structured graphene metamaterial selective absorbers for high efficiency and
2 omnidirectional solar thermal energy conversion. *Nature communications*. 2020;11:1-10.
- 3 [12] Wang W, Wen H, Huan X, Shi J, Li Z, Su J, et al. Single layer WO_x films for efficient solar selective absorber. *Materials*
4 & Design. 2020;186:108351.
- 5 [13] Yang Y, Wang T, Yao T, Li G, Sun Y, Cao X, et al. Preparation of a novel TiN/TiN_xO_y/SiO₂ composite ceramic films on
6 aluminum substrate as a solar selective absorber by magnetron sputtering. *Journal of Alloys and Compounds*.
7 2020;815:152209.
- 8 [14] Bello M, Shanmugan S. Achievements in mid and high-temperature selective absorber coatings by physical vapor
9 deposition (PVD) for solar thermal Application-A review. *Journal of Alloys and Compounds*. 2020;839:155510.
- 10 [15] Herrera-Zamora DM, Lizama-Tzec FI, Santos-González I, Rodríguez-Carvajal RA, García-Valladares O, Arés-Muzio O, et
11 al. Electrodeposited black cobalt selective coatings for application in solar thermal collectors: Fabrication, characterization,
12 and stability. *Solar Energy*. 2020;207:1132-45.
- 13 [16] Han Z, Liu K, Li G, Zhao X, Shittu S. Electrical and thermal performance comparison between PVT-ST and PV-ST systems.
14 *Energy*. 2021;237:121589.
- 15 [17] Bahadori MN. Passive cooling systems in Iranian architecture. *Scientific American*. 1978;238:144-55.
- 16 [18] Lee D, Go M, Son S, Kim M, Badloe T, Lee H, et al. Sub-ambient daytime radiative cooling by silica-coated porous
17 anodic aluminum oxide. *Nano Energy*. 2021;79:105426.
- 18 [19] Huang Z, Ruan X. Nanoparticle embedded double-layer coating for daytime radiative cooling. *International Journal*
19 *of Heat and Mass Transfer*. 2017;104:890-6.
- 20 [20] Li D, Liu X, Li W, Lin Z, Zhu B, Li Z, et al. Scalable and hierarchically designed polymer film as a selective thermal emitter
21 for high-performance all-day radiative cooling. *Nature Nanotechnology*. 2021;16:153-8.
- 22 [21] Zhao D, Aili A, Zhai Y, Xu S, Tan G, Yin X, et al. Radiative sky cooling: Fundamental principles, materials, and applications.
23 *Applied Physics Reviews*. 2019;6.
- 24 [22] Wang X, Liu X, Li Z, Zhang H, Yang Z, Zhou H, et al. Scalable flexible hybrid membranes with photonic structures for
25 daytime radiative cooling. *Advanced Functional Materials*. 2020;30:1907562.
- 26 [23] Bijarniya JP, Sarkar J, Maiti P. Review on passive daytime radiative cooling: Fundamentals, recent researches,
27 challenges and opportunities. *Renewable and Sustainable Energy Reviews*. 2020;133:110263.
- 28 [24] de Paula CH, Duarte WM, Rocha TTM, de Oliveira RN, Maia AAT. Optimal design and environmental, energy and
29 exergy analysis of a vapor compression refrigeration system using R290, R1234yf, and R744 as alternatives to replace
30 R134a. *International Journal of Refrigeration*. 2020;113:10-20.
- 31 [25] Tso CY, Chan KC, Chao CYH. A field investigation of passive radiative cooling under Hong Kong's climate. *Renewable*
32 *Energy*. 2017;106:52-61.
- 33 [26] Hong X, Leung MKH, He W. Effective use of venetian blind in Trombe wall for solar space conditioning control. *Applied*
34 *Energy*. 2019;250:452-60.
- 35 [27] Ono M, Chen K, Li W, Fan S. Self-adaptive radiative cooling based on phase change materials. *Optics Express*.
36 2018;26:A777-A87.
- 37 [28] Matsuta M TS, Ito H. 1987 Solar heating and radiative cooling using a solar collector-sky radiator with a spectrally
38 selective surface. *Solar Energy*. 1987;39(3):183-6.
- 39 [29] Hu M, Pei G, Wang Q, Li J, Wang Y, Ji J. Field test and preliminary analysis of a combined diurnal solar heating and
40 nocturnal radiative cooling system. *Applied Energy*. 2016;179:899-908.
- 41 [30] Hu M, Zhao B, Ao X, Su Y, Pei G. Parametric analysis and annual performance evaluation of an air-based integrated
42 solar heating and radiative cooling collector. *Energy*. 2018;165:811-24.
- 43 [31] Chen Z, Zhu L, Li W, Fan S. Simultaneously and Synergistically Harvest Energy from the Sun and Outer Space. *Joule*.
44 2019;3:101-10.
- 45
46
47
48
49
50
51
52
53
54
55
56
57
58
59
60
61
62
63
64
65

- 1 [32] Hu M, Zhao B, Suhendri, Cao J, Wang Q, Riffat S, et al. Feasibility of realizing daytime solar heating and radiative
2 cooling simultaneously with a novel structure. *Sustainable Cities and Society*. 2021;74.
- 3 [33] Agathokleous R, Barone G, Buonomano A, Forzano C, Kalogirou SA, Palombo A. Building façade integrated solar
4 thermal collectors for air heating: experimentation, modelling and applications. *Applied Energy*. 2019;239:658-79.
- 5 [34] Fu H, Li G, Li F. Performance comparison of photovoltaic/thermal solar water heating systems with direct-coupled
6 photovoltaic pump, traditional pump and natural circulation. *Renewable Energy*. 2019;136:463-72.
- 7 [35] Wang Y, Ji J, Sun W, Yuan W, Cai J, Guo C, et al. Experiment and simulation study on the optimization of the PV direct-
8 coupled solar water heating system. *Energy*. 2016;100:154-66.
- 9 [36] Zhao D, Aili A, Zhai Y, Lu J, Kidd D, Tan G, et al. Subambient Cooling of Water: Toward Real-World Applications of
10 Daytime Radiative Cooling. *Joule*. 2019;3:111-23.
- 11 [37] Hu M, Zhao B, Ao X, Zhao P, Su Y, Pei G. Field investigation of a hybrid photovoltaic-photothermic-radiative cooling
12 system. *Applied Energy*. 2018;231:288-300.
- 13 [38] Hu M, Zhao B, Ao X, Feng J, Cao J, Su Y, et al. Experimental study on a hybrid photo-thermal and radiative cooling
14 collector using black acrylic paint as the panel coating. *Renewable Energy*. 2019;139:1217-26.
- 15 [39] Wang Q, Li J, Yang H, Su K, Hu M, Pei G. Performance analysis on a high-temperature solar evacuated receiver with
16 an inner radiation shield. *Energy*. 2017;139:447-58.
- 17
18
19
20
21
22
23
24
25
26
27
28
29
30
31
32
33
34
35
36
37
38
39
40
41
42
43
44
45
46
47
48
49
50
51
52
53
54
55
56
57
58
59
60
61
62
63
64
65